OXFORD

Human Molecular Genetics, 2022, Vol. 31, 24, 4217–4227

https://doi.org/10.1093/hmg/ddac174
Advance access publication date 28 July 2022
Original Article

ETS1 loss in mice impairs cardiac outflow tract septation via a cell migration defect autonomous to the neural crest

Lizhu Lin[1,†], Antonella Pinto[2,†], Lu Wang[1,†], Kazumi Fukatsu[1], Yan Yin[1], Simon D. Bamforth[3], Marianne E. Bronner[4], Sylvia M. Evans[5], Shuyi Nie[6], Robert H. Anderson[3,†], Alexey V. Terskikh[2,†] and Paul D. Grossfeld[1,7,†*]

[1]Department of Pediatrics, UCSD School of Medicine, La Jolla, CA 92093, USA
[2]Department of Biology, Sanford-Burnham-Prebys Institute of Medical Discovery, La Jolla, CA 92037, USA
[3]Cardiovascular Research Centre, Institute of Genetic Medicine, Newcastle University, Newcastle upon Tyne NE1 3BZ, UK
[4]Department of Biology, California Institute of Technology, Pasadena, CA 91125, USA
[5]Department of Pharmacology, Skaggs School of Pharmacy and Pharmaceutical Sciences, UCSD, La Jolla, CA 92093, USA
[6]Department of Biology, Georgia Institute of Technology, Atlanta, GA 30332, USA
[7]Division of Cardiology, Rady Children's Hospital, San Diego, CA 92123, USA

*To whom correspondence should be addressed at: 3020 Children's Way, MC 5004, San Diego, CA 92123, USA. Email: pgrossfeld@health.ucsd.edu

†These authors contributed equally.

Abstract

Ets1 deletion in some mouse strains causes septal defects and has been implicated in human congenital heart defects in Jacobsen syndrome, in which one copy of the *Ets1* gene is missing. Here, we demonstrate that loss of *Ets1* in mice results in a decrease in neural crest (NC) cells migrating into the proximal outflow tract cushions during early heart development, with subsequent malalignment of the cushions relative to the muscular ventricular septum, resembling double outlet right ventricle (DORV) defects in humans. Consistent with this, we find that cultured cardiac NC cells from *Ets1* mutant mice or derived from iPS cells from Jacobsen patients exhibit decreased migration speed and impaired cell-to-cell interactions. Together, our studies demonstrate a critical role for ETS1 for cell migration in cardiac NC cells that are required for proper formation of the proximal outflow tracts. These data provide further insights into the molecular and cellular basis for development of the outflow tracts, and how perturbation of NC cells can lead to DORV.

Introduction

Proper heart development requires precise specification and migration of cardiac neural crest (NC) cells (1–5). Cardiac NC cells are essential for the remodeling of the extra-pericardial arterial channels and septation of the outflow tract (OFT). This remodeling not only separates the pulmonary and systemic circulations, but also underlies the development of the arterial valves (6,7). During early embryonic development, cardiac crest cells arise from the lateral folds of the caudal hindbrain, located between the otic placodes and the third somite. Beginning on E8.5 in the mouse, NC cells undergo an epithelial–mesenchymal transition, to emigrate from the neural tube and migrate through the posterior pharyngeal arches to the developing heart. In animal models, impairment of cardiac crest function causes congenital heart defects (CHDs) (5,7).

ETS1, a member of the ETS family of transcription factors (8), has been implicated as a causal factor in CHDs. As case in point, multiple lines of evidence suggest that ETS1 is the cause of CHDs in Jacobsen syndrome: (1) all patients with Jacobsen syndrome and CHDs have a deletion that spans the *Ets1* gene (9); (2) the cardiac 'critical region', as defined by interstitial deletions in distal 11q is ∼1 megabase and contains only seven annotated genes including *Ets1* (10); (3) studies in *Ciona intestinalis* and *Drosophila* suggest an important role for ETS1 in heart development, specifically in determining cardiac cell fate and migration (11,12) and (4) at least one patient has been identified with double outlet right ventricle (DORV) and hypoplasia of the left ventricle with a *de novo* loss-of-function frameshift mutation in the *Ets1* gene (13).

Previous studies have reported that deletion of *Ets1* causes septal defects in mice in a C57BL/6 background (10,14,15). The mechanism(s) underlying how deletion of *Ets1* causes CHDs remains unknown. In this study, we trace the migration pattern of murine cardiac NC cells *in vivo* during early stages of heart development not previously studied. *Ets1* is highly expressed in pre-migratory and migrating cardiac crest cells and its deletion causes migration defects, leading to impaired OFT remodeling. Not only does loss of ETS1 results in a decrease in the number of migrating cardiac NC cells populating the proximal OFT cushions, but also causes a failure to build the muscular shelf in the roof of the developing right ventricle required for normal septation of the proximal OFTs, resulting in a DORV phenotype not previously described. We demonstrate this is due to impaired muscularization of the cushions, leaving a fibrous outlet septum and continuity between the aortic and pulmonary valvar leaflets, with a ventricular septal defect in the subaortic position. We also observe a bisinuate aortic valve in three out of four *Ets1* knockout (KO) mutant embryos,

Received: February 24, 2022. **Revised:** July 22, 2022. **Accepted:** July 26, 2022

indicative of a defect in the development of the intercalated valvar swellings. *In vitro* studies using cultured cardiac crest cells demonstrate that loss of ETS1 causes decreased migration velocity and impaired cell-to-cell interactions. *In vivo* studies demonstrate increased N-cadherin expression in ETS1-deficient neural crest cells, a likely direct downstream target of ETS1, and suggestive that N-cadherin may be a genetic modifier of the ETS1 gene affecting the development of CHDs. We also show for the first time that conditional deletion of *Ets1* in the NC recapitulates the global *Ets1* mutant cardiac phenotype, consistent with a NC-autonomous mechanism underlying the cardiac phenotype. Finally, we demonstrate that NC cells derived from iPS cells lacking one copy of the *Ets1* gene from patients with Jacobsen syndrome and congenital heart disease display NC cell migration defects, consistent with our murine studies, also providing a likely molecular basis for the incomplete penetrance of the cardiac phenotype in patients with Jacobsen syndrome. Together, the results demonstrate a critical role for ETS1 in cardiac NC cells for normal heart development, extending the results of previous studies and highlighting the fact that a subset of cardiac NC cells is required for formation of the proximal outflow cushions and subsequent OFT septation.

Results

Global deletion of *Ets1* in a pure C57BL/6J background causes DORV

Ets1 is highly expressed in cardiac NC cells during early murine development (10). Moreover, deletion of *Ets1* in C57BL/6J mice causes septal defects (10,14). To better define the three-dimensional anatomy of the heart defects, we performed cardiac MRIs on E15.5 mouse embryos lacking ETS1 compared with control hearts. As shown in Figure 1, there is exclusive origin of the aorta from the right ventricle, giving the ventriculo-arterial connection of DORV (Fig. 1A and B). Of the four E15.5 *Ets1* KO hearts analysis by MRIs, three of them exhibited DORV phenotypes and one exhibited an overriding aorta phenotype. In addition, serial section analysis through the OFTs in E14.5 embryonic hearts demonstrated all four *Ets1* KO E14.5 hearts have DORV. Three out of four *Ets1* KO embryos (Fig. 1D and F) analyzed have a bisinuate and bi-leaflet aortic valves, whereas a trileaflet aortic valve was observed in all six control hearts (Fig. 1C and E). Combined with the observed reduction in NC cells at the aortic valve, our results indicate that ETS1 is required in cardiac crest cells for proper septation of the OFT. In addition, heterozygous ETS1 KO mice demonstrate a patch of white fur on their abdomen, consistent with a NC cell defect as described previously (14).

Loss of ETS1 causes NC migration defects in *Ets1*$^{-/-}$ mutant mice

We first examined the role of ETS1 in cardiac NC migration. To track the cardiac crest, we used *Pax3Cre;tdTomato* reporter mouse embryos (16). Pax3Cre is an established reporter that is expressed in the dorsal neural tube and migrating NCCs reflecting the endogenous expression of the NC transcription factor Pax3 (17). The fidelity of the reporter was confirmed by immunohistochemistry analysis against ETS1. We observed co-expression of ETS1 in *Pax3Cre–Tdtomato* expressing cardiac NC cells migrating from the neural tube toward the developing heart (Supplementary Material, Fig. S1). Next, we compared cardiac crest cells from control and *Ets1* KO embryos at pre-migratory, migratory and post-migratory stages (E8.5–E11.5) using the *Pax3Cre;tdTomato* mouse embryos. Three embryos from each genotype and developmental stage were analyzed. The results demonstrate that prior to neural tube closure at E8.5, a similar number of *tdTomato*-expressing pre-migratory cardiac NC cells are present in the neural folds of both *Ets1* KO and control embryos (Fig. 2A and B). At E9.5, when the neural tube closes and cardiac NC cells have started migration, *tdTomato*-expressing cells are observed in the developing OFT of control embryos (Fig. 2C). Despite the migration of cardiac crest cells from the dorsal neural tube in *Ets1* KO embryos, there were fewer *tdTomato* cNCCs in the developing cardiac OFT in *Ets1* KO mutant (Fig. 2D) compared to control embryos, suggesting a delay of NC migration into the heart. At E10.5, in the control (Fig. 2E), the *tdTomato* cNCCs are present in the developing OFT cushions (Fig. 2E, arrows), whereas in the *Ets1* KO mutant, there is a nearly complete absence of t*dTomato* cells in the proximal component of the OFT cushions (Fig. 2F). The lack of *tdTomato* cNCCs in the proximal outflow cushion persists at E11.5, although less severe compared to earlier stages, consistent with delayed migration. In the control, the *Pax3Cre–tdTomato* expressing cells are present throughout the proximal–distal axis of outflow cushions (Fig. 2G), whereas in the *Ets1* KO mutant, cardiac crest cells are found predominantly in the distal outflow cushions, with fewer *Pax3Cre–tdTomato*-expressing cells in the proximal cushions (Fig. 2H). Quantitation of *tdTomato* cells in the OFT for the sections shown in Figure 2C–H from E9.5 through E11.5 is shown in Figure 2I.

These results were further confirmed by immunohistochemistry analysis against another NC transcription factor, SOX10. SOX10 is critical for specification of NC cells and is a direct downstream target of ETS1 in chick (18). In control embryos, most of the migratory *Pax3Cre–tdTomato* expressing cells co-expressed SOX10 protein (Fig. 3A and A′). They are observed streaming in a linear fashion from the neural tube toward the heart. In *Ets1* KO mutant embryos, there was a loss of the linear migratory pattern (Fig. 3B and B′′). Most of the *tdTomato* cells lacked SOX10 expression, suggesting that ETS1 plays a conserved regulatory role in the transcription of SOX10 in mice, and that loss of SOX10 expression contributes to the migration defects of *Ets1* KO NCCs.

Loss of ETS1 causes decreased migration velocity and abnormal cell adhesion in cultured cardiac NC cells

To fully characterize their migration properties, we performed time-lapse imaging of cultured cardiac crest cells as described previously (19) using a *Pax3Cre;tdTomato* reporter strain from E8.5 *Ets1* KO and control embryos. To analyze cell migration, we explanted the neural tube from the somite 1–3 region of E8.5 mouse embryos, which was then cultured for 24 h. We then followed the migration of individual cardiac crest cells by imaging at 10 min intervals for 3 h (see Materials and Methods for details). The speed of migration in the *Ets1* KO mutants was significantly decreased compared to controls (0.19 μm/min vs 0.8 μm/min vs $P < 0.0001$, Fig. 4). Since the loss of ETS1 results in a disruption of the linear stream pattern of migration, we also assessed cell-to-cell interactions during their migration (Table 1). In control cells, 8.5% of cells make contact and a large percentage of them (68.8%) separate within 2 h. A slightly higher percentage of cardiac crest cells from *Ets1* KO mutant embryo made cell–cell contacts (12.7%), and more strikingly, 81% of those contacts failed to separate within 2 h. Taken together, these results suggest that cardiac crest from *Ets1* KO mutants have increased cell–cell adhesion compared to controls. N-cadherin plays a crucial role in NC migration (20,21) and previous studies have demonstrated that N-cadherin over-expression in the chick blocked their migration

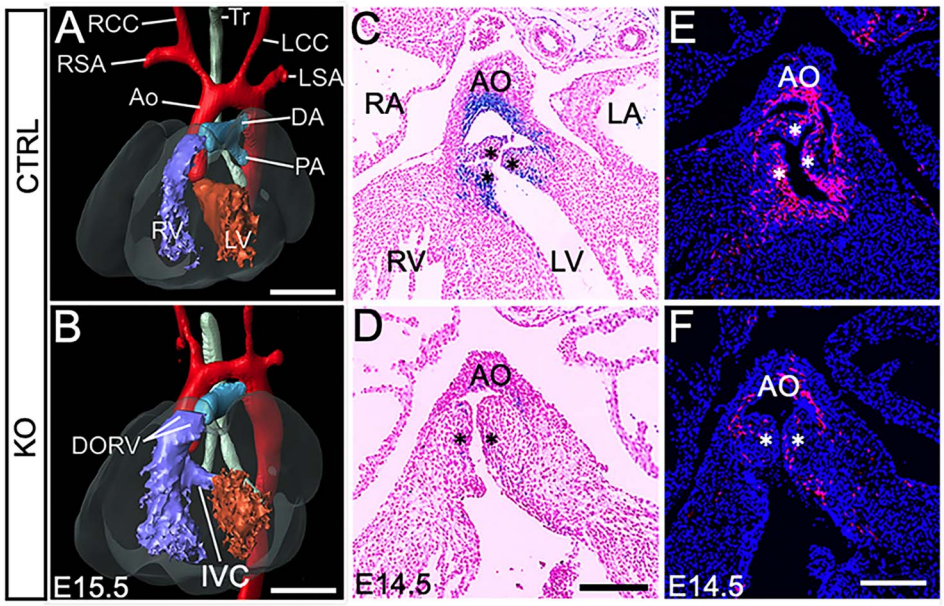

Figure 1. *Ets1* KO mutant hearts exhibit DORV and a bisinuate (two leaflet) aortic valve. (**A**, **B**) Cardiac MRI studies demonstrate the *Ets1* KO mutant heart DORV phenotype. Control (A), Ets1 mutant (B). LCC, left common carotid; LSA, left subclavian artery; PA, pulmonary artery; RCC, right common carotid; RSA, right subclavian artery and Tr, trachea. Scale bars: 500 μm. (**C**–**F**) Serial section analysis through the OFTs in E14.5 hearts revealed a two leaflet (bisinuate) aortic valve in three out of four KO embryos analyzed (asterisks). Control hearts (C, E) and *Ets1* mutant (D, F). NC cells are stained with LacZ in C and D (in blue), and tdTomato in E and F (in magenta). Scale bars: 200 μm.

Table 1. Quantitative assessment of cell-to-cell interaction in cultured cardiac NC cells

	Control	***ETS-1* KO**
Total number of cells	189	166
Number of cells that make contact	16	21
Number of cells that make contact and then separate (over 2 h)	11 (68.8%)	4 (19.0%)
Number of cells that make contact but do not separate (over 2 h)	5 (31.2%)	17 (81.0%)

(20,21). We hypothesized that the cell migration defect observed *in vivo* may result from impaired expression of N-cadherin. To test this, we assessed N-cadherin expression by immunofluorescence on sections from E8.5 and E9.5 embryos, corresponding to the early migration stage. The results show that N-cadherin protein levels were markedly increased in the migratory NCCs in *Ets*1 KO mutants compared to controls (Fig. 5A–D), indicating a potential molecular basis for the migration defect caused by loss of ETS1. Furthermore, bioinformatics analysis of the promoter region of the mouse N-cadherin gene identified three likely ETS binding sites, suggesting that N-cadherin is a direct downstream target of ETS1 (Fig. 5E).

Loss of ETS1 impairs myocardialization in the developing OFT

Myocardialization is the process by which cardiac myocytes from the OFT myocardium invade the OFT cushions in order to complete the process of septation, and for the subsequent formation of the subpulmonary muscular infundibulum. To investigate the role of ETS1 in myocardialization, we performed immunofluorescent analysis using an antibody against alpha-actinin, as a marker for cardiac myocytes. In E13.5 control embryos, cardiac myocytes in the myocardium of the OFT are seen invading the OFT cushions (Fig. 6A and A′). They are in close proximity to *Pax3Cre–tdTomato* expressing cNCCs. In *Ets*1 KO mutants, there was a gap between cardiac myocytes and *Pax3Cre–tdTomato* expressing cardiac crest cells, indicative of impaired myocardialization at E13.5 (Fig. 6B and B′′). By E15.5 the muscularization of OFT cushions is complete in the control embryos, with the newly produced myocardium forming the free-standing subpulmonary infundibular sleeve. By this stage, the *Pax3Cre–tdTomato* are almost completely surrounded by cardiomyocytes (Fig. 6C and C′), persisting as the fibrous tendon of the infundibulum. In the *Ets*1KO mutant, in contrast, there were far fewer cardiomyocytes in contact with *Pax3Cre–tdTomato* cell, with the cardiac NC cells persisting as a fibrous outlet septum in the setting of DORV (Fig. 6D and D′). By E18.5, while there was an infundibular sleeve consisting of cardiac myocytes in the control (Fig. 7A and A′), the sleeve was severely reduced in *Ets*1 KO mutant. Instead of the tendon of the infundibulum, the fibrous outlet septum now produced continuity between leaflets of the aortic and pulmonary valves, which were in a side-by-side orientation (Fig. 7B and B′). Interestingly, this structure appears to be the same as the cartilaginous structure described previously by Gao *et al.* (14).

NC-specific conditional deletion of *Ets1* recapitulates the global KO cardiac phenotype

Previous studies have implicated a NC cell-autonomous mechanism by which loss of ETS1 causes septal defects. To examine the role of ETS1 specifically in the NC, we generated an *Ets1* NC-specific mutant mouse line in which *Ets1* is deleted via Cre-LoxP-mediated recombination (Supplementary Material, Fig. S2). The original *Ets1* floxed mice we obtained were in a mixed genetic background. We bred the mice with C57BL/6J mice for

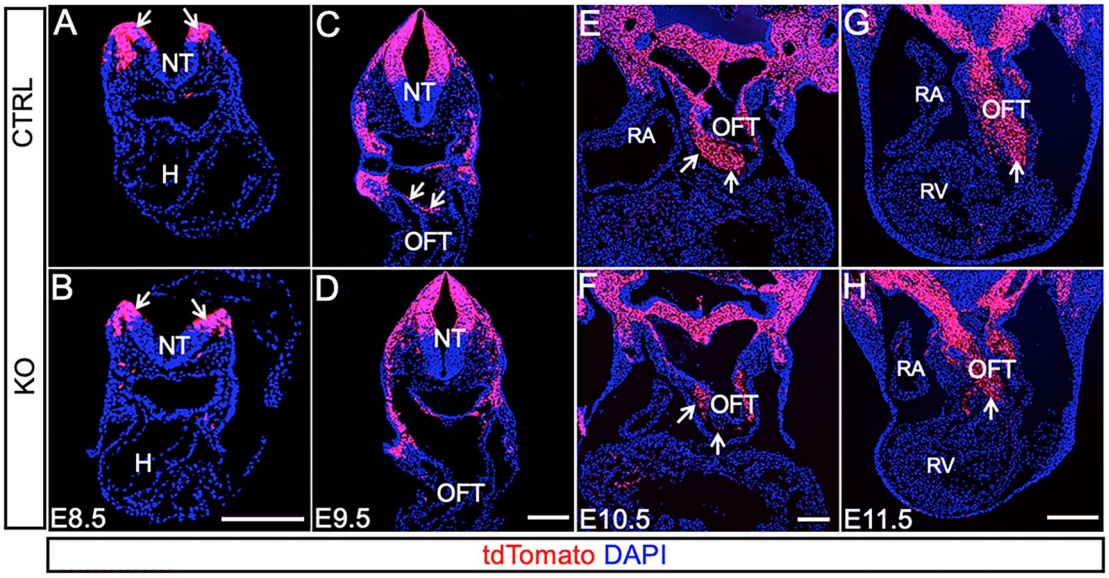

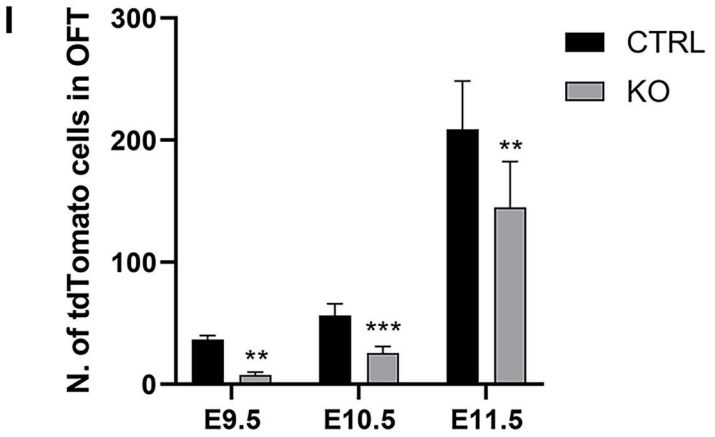

Figure 2. Cardiac NC cells in sections from embryos with *Pax3Cre;tdTomato* reporter. At E8.5, the *tdTomato* labeled NCCs are present in the neural fold in both controls and *Ets1* KO mutants (**A**, **B**, arrows). At E9.5, the *tdTomato-labeled* cNCCs are present in the developing cardiac OFT in controls (**C**, arrows). There are fewer *tdTomato* cNCCs in the developing cardiac OFT in the *Ets1* KO mutant (**D**). At E10.5, the *tdTomato* cNCCs have populated the developing OFT cushions in controls (**E**, arrows), but there are fewer *tdTomato*-labeled cNCCs in the outflow cushions in the *Ets1* KO mutants (**F**, arrows). At E11.5, there are abundant *tdTomato* cNCCs in the proximal outflow cushions in controls (**G**, arrows), but in the *Ets1* KO mutants, the *tdTomato* cNCCs are observed only in the distal and intermediate outflow cushions (**H**, arrow), and not in the proximal cushion. Scale bars: 100 μm (**I**), quantitation of *tdTomato* cNCCs in the OFT shown in the sections. The number of *tdTomato* cNCCs in the OFT in controls and *Ets1* KO mutants was counted, demonstrating decreased *tdTomato* cNCCs in the developing cardiac OFT in the *Ets1* KO mutant from E9.5 through E11.5, compared to controls. $^{**}P < 0.01$; $^{***}P < 0.001$.

12 more generations and then used a *Pax3Cre* driver to delete *Ets1* specifically in NC cells (17). Analysis of *Pax3Cre;Ets1* conditional knockout (cKO) embryos revealed DORV (Fig. 8B and D) with incomplete penetrance. Of the eight *Pax3Cre;Ets1* conditional deletion embryos analyzed, four of them exhibited DORV (Supplementary Material, Table S1). To determine if the 50% penetrance could be due to inefficient expression of the Cre leading to incomplete deletion of the gene, we assessed ETS1 protein expression by immunohistochemistry analysis on sections from E10.5 *Pax3Cre;Ets1* conditional deletion mutants and *Pax3Cre* controls. ETS1 is co-expressed with SOX10 in control embryos (Supplementary Material, Fig. S3A and A′). In contrast, there was a nearly complete absence of ETS1 protein signal in SOX10 expressing cardiac crest cells in *Pax3Cre;Ets1* conditional deletion mutants (Supplementary Material, Fig. S3B and B′), demonstrating efficient deletion of the floxed allele by E10.5. To test further for efficiency of deletion we used a *Sox2Cre* driver to generate a global deletion of *Ets1* using the *Ets1* floxed allele. *Sox2Cre*-mediated deletion of the *Ets1*-floxed allele resulted in DORV with complete penetrance, reproducing the global KO phenotype (data not shown). These results indicate an early temporal requirement for ETS1 for normal cardiac crest function. There is likely variability in the exact timing of the deletion of the *Ets1*-floxed allele, such that it is deleted prior to the time it is required in only a subset of embryos.

Generation of NC cells from human-induced pluripotent stem cells (iPSCs) from patients with Jacobsen syndrome and congenital heart disease

Our studies in mice demonstrate a clear link between DORV and the deficit of Ets1 in the cardiac NC. To explore the effect of loss of ETS1 in NC migration in human patients with congenital heart disease, we generated NC cells from human iPSCs from three healthy subjects and two patients with Jacobsen syndrome and hypoplastic left heart syndrome (HLHS): patient

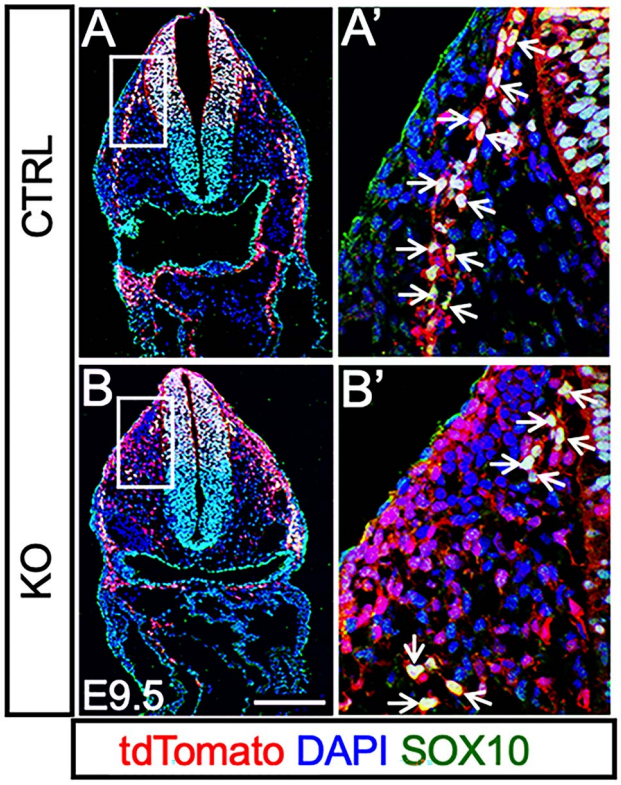

Figure 3. Loss of ETS1 causes NCCs migration defects. (**A**–**B**′) Immunostaining for SOX10 protein (green), a marker for migrating NCCs, in sections from E9.5 control and *Ets1* KO embryos with *Pax3Cre;tdTomato* reporter. In control (**A**, **A**′ arrows), the Pax3-Cre-expressing migrating NCCs cells are co-expressed with SOX10 protein and the *tdTomato* positive-expressing SOX10 cells are observed in a linear configuration from the neural tube toward the developing heart. However, in *Ets1* KO mutants the number of the *tdTomato* positive-expressing SOX10 cells is markedly reduced (**B**, **B**′ arrows), and the linear migration pattern is disrupted. Furthermore, most of the *tdTomato* positive-expressing cells lacking SOX10 expression are located more peripherally. Scale bars: 100 μm.

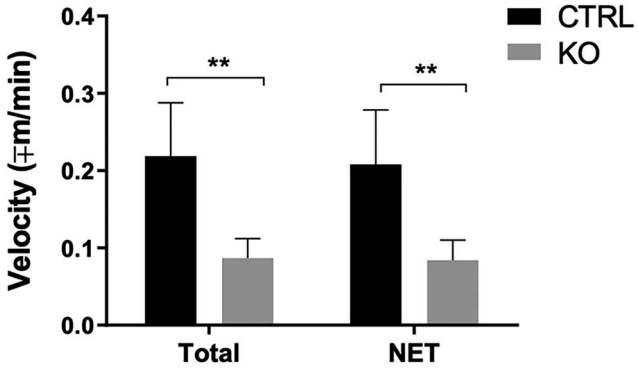

Figure 4. Time-lapse image analysis of explanted cultured cNCCs from controls and *Ets1* KO mutant embryos. Quantitation of migration velocity of cNCCs. Total, total distance and NET, net distance traveled. The data represent the mean ± SD of seven independent experiments of cultured cNCCs from control and *Ets1* KO mutant embryos ($n = 5$). Statistical analysis was performed by two-tailed unpaired *t*-test at confident level of 95%. $^{***}P < 0.001$.

8389 has a 14.0 Mb terminal deletion and multiple craniofacial defects; patient 192 has an 8.0 Mb terminal deletion and mild hypertelorism (Supplementary Material, Table S2). To characterize iPSC-derived NCCs, we employed a neurosphere-based migration method, as published previously (22–25). When the iPSC-derived neurospheres were plated on Matrigel, a permissive substrate for NC cells, a migratory cell population emerged mimicking early events of NC delamination from the dorsal neural tube. These migratory cells expressed known NC markers, including SOX10, SOX9, Nestin and Pax3 and downregulated the expression of pluripotency markers such as OCT4 and SOX2 in both control and patient cells (Supplementary Material, Fig. S4). Upon neuralization, expression of the pluripotency marker OCT4 was suppressed, while SOX2 levels were reduced by 70% in both control and patient cells (Supplementary Material, Fig. S4).

Loss of ETS1 negatively affects the migration profile of hiPSC-derived NC cells

Based on our data from ETS1 KO mice indicating a NC cell migration defect, we assessed the migratory performance of the hiPSC-derived NCCs *in vitro*. We studied the ability of all the iPSC-NCCs lines to invade a matrix and move towards a central cell-free zone. A 3-D matrix approach was chosen to recapitulate the best *in vivo* environment. Cell invasion was quantified by obtaining snapshot images with an automated microscope every 24 h. By measuring the number of cells in the cell-free detection zone over time, we observed an impaired migratory phenotype of NC derived from iPSCs from the two patients compared to the three controls (Fig. 9). At 48 h, NC cells from the two patients had a slower migration rate compared to wild-type controls. To further test the possibility that the lack of Ets1 in migratory NC cells was responsible for the migration defects, we silenced the ETS1 gene in control and patient iPSC-NCCs using siRNA for 72 h. ETS1-silenced cells showed a decrease in ETS1 mRNA (Supplementary Material, Fig. S5). This negatively affected the migration rate of cells into the extracellular matrix, resulting in a reduction of cell counts in the cell-free zone (Fig. 10 and Supplementary Material, Fig. S6), consistent with our findings in mice that loss of ETS1 is sufficient to impair NC cell migration.

Discussion

Global deletion of ETS1 in C57/B6 mice caused ventricular septal defects, which is the most common CHD that occurs in Jacobsen syndrome, thus identifying the ETS1 transcription factor as a candidate gene for causing CHDs in this setting (9,10,14). Previous studies have led to the hypothesis that the heart defects in ETS1 KO mice were due to impaired migration of NC cells involving the endocardial cushions (14,15). Our studies endorse and extend these observations, providing additional insights regarding the anatomical background of the lesions produced.

In this study, we performed a 3-D analysis of ETS1 KO embryonic hearts, which revealed DORV with a subaortic intraventricular communication and side-by-side arterial trunks. To date, we have never observed common arterial trunk in ETS1 KO mice, suggesting that loss of ETS1 affects OFT septation but NOT the separation of the distal OFT into the aorta and pulmonary trunk. It is unknown if, in mammals, there are distinct subsets of cardiac NC cells that are required for these two developmental processes, or if a common subset of NC cells can execute both the functions.

In support of the idea that ETS1 is important for cardiac crest migration, here we demonstrate that ETS1 KO mice have decreased numbers of cardiac NC cells in the developing proximal OFT cushions, consistent with delayed migration. This is detectable as early as E9.5 and is consistent with previous studies

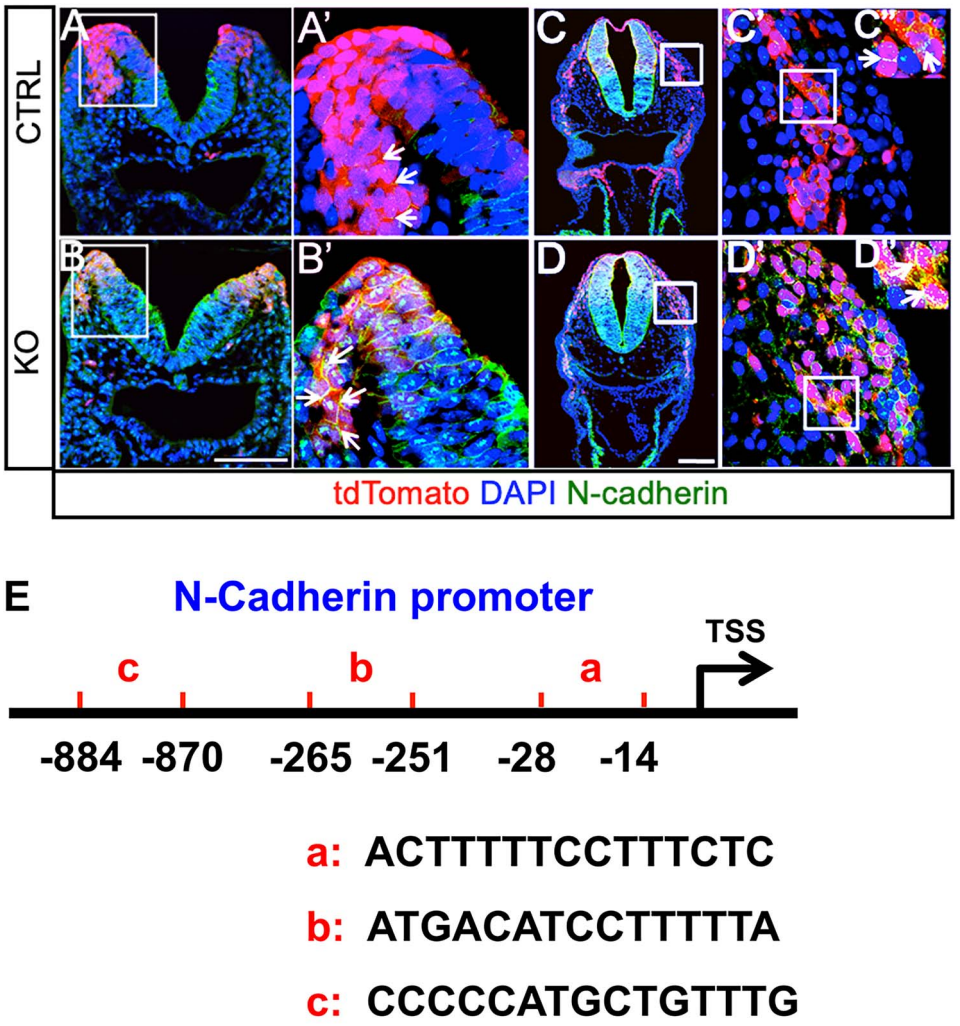

Figure 5. Immunofluorescence analysis of sections from controls and *Ets1* KO mutants with *Pax3Cre;R26R-tdTomato* reporter. N-cadherin staining demonstrates upregulation of N-cadherin expression in migratory NCCs in *Ets1* KO mutant at E8.5 (**A′**, **B′**, arrows) and E9.5 (**C′**, **D′**, arrows). *Pax3Cre–tdTomato* (red), anti-N-cadherin (green), nucleus (DAPI, blue). Scale bars: 100 μm. (**E**) Potential binding sites of ETS1 in the promoter regions of N-cadherin predicted by JASPAR (a, b and c, three potential ETS1 binding sites).

that have demonstrated a critical role for the proximal OFT cushions in the development of the ventricular OFTs (26). Specifically, our findings implicate a critical role for ETS1 in building the shelf in the roof of the right ventricle that subsequently allows for the aorta to achieve its connection with the left ventricle. Of note, we also performed cell proliferation and apoptosis studies on E11.5 ETS1 global KO mice, and there was no difference compared to wild-type controls (data not shown). In addition, it is possible that ectopic migration of cardiac NC cells could also contribute to the decreased cardiac NC cells observed in the proximal cushions. Although not systematically studied, we did observe weak expression of SOX10 in the optic node in ETS1 global KO mice (data not shown), suggestive of ectopic migration in a small subset of cardiac NC cells.

Interestingly, surgical repair of this form of DORV is performed utilizing the procedure (27) in which a tunnel is built such that the interventricular communication is used to place the aortic root in continuity with the left ventricular cavity. In addition, three out of four ETS1 KO mice analyzed have a bisinuate aortic valve with decreased NC cells in the valvar leaflets, consistent with previous studies demonstrating a critical role for cNCCs in arterial valvar development (6). In addition to decreased numbers of NCCs in the proximal cushions prior to the time of OFT septation, ETS1 KO mice demonstrate abnormal myocardialization, resulting in the presence of a fibrous outlet septum, with continuity between the leaflets of the aortic and pulmonary valves. Impaired myocardialization suggests that normally cardiac crest cells populating the proximal OFTs generate a yet to be identified factor(s) that is required for cardiac myocyte migration to the cushions.

Our studies implicate a unique subset of cardiac crest cells that are required for septation of the OFTs, independent of those required for separation of the distal OFT into the pulmonary trunk and aorta. It is unclear whether this failure may be specifically due to decreased migration of a multifunctional population of cardiac crest cells to the proximal cushions, which can execute separation of the OFTs. Alternatively, there may be a unique subset of predetermined cardiac crest that populates the proximal cushions and are required for myocardialization. Consistent with this model, recent studies in chick by Gandhi *et al.* indicate that there are distinct functional populations of pre-migratory cardiac crest cells that exist in the left and right sides of the neural folds (28), such ablation of left versus right-sided neural folds gives rise predominantly to DORV versus common arterial trunk, respectively.

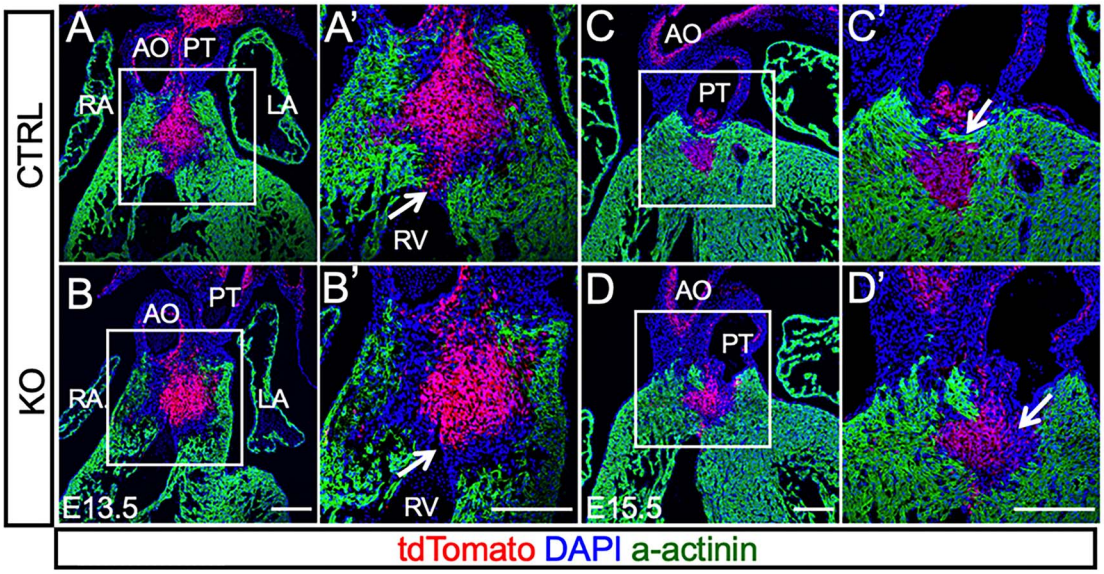

Figure 6. Immunofluorescence analysis of sections from controls and *Ets1* KO mutants with the *Pax3Cre;tdTomato* reporter. Alpha-actinin staining demonstrated cardiomyocytes adjacent to and protruding into *tdTomato* positive cNCCs in the OFT cushion in control E13.5 embryos (**A**). In the mutant, the cardiac myocytes are separated from the *tdTomato* positive cNCCs (**B**). **A′** and **B′** show higher magnification images boxed in A and B. By E15.5, the *tdTomato* positive cNCCs in OFT cushions are fully surrounded by cardiomyocytes, demonstrated completion of muscularization of OFT cushions (**C**), but in the *Ets1* KO mutant, there were markedly fewer cardiomyocytes in contact with *tdTomato* positive cNCCs in the OFT cushion, indicating impaired muscularization. a-Actinin (green), nucleus (DAPI, blue). Scale bars: 100 μm.

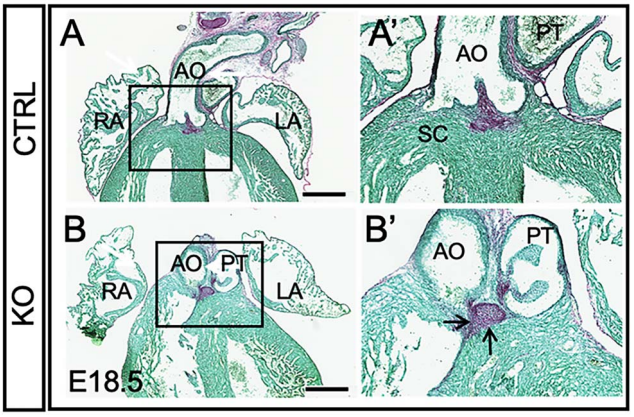

Figure 7. Sirius Red analysis of sections from controls and *Ets1* KO mutants. In E18.5 *Ets1* KO mutants, the supraventricular crest (SC) in control hearts (**A**, **A′**) was replaced with fibrotic tissue (**B**, **B′**, arrows), with continuity between the aortic and pulmonary valve leaflets. Scale bars: 500 μm.

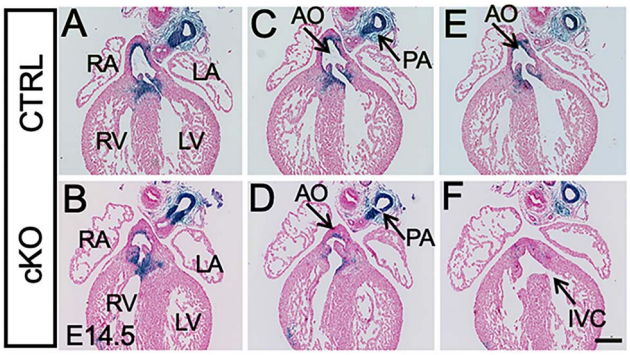

Figure 8. Histological analysis of cardiac defects in E14.5 *Pax3Cre; Ets1* cKO hearts. Pax3Cre; R26R-LacZ-stained showing contribution of cNCCs to OFT cushions, aortic valve leaflets and pulmonary trunk in an E14.5 control heart (**A**, **C**, **E**) and a *Pax3Cre;Ets1* cKO heart (**B**, **D**, **F**) demonstrating the DORV phenotype: the aorta is aligned with the right ventricle with an interventricular communication (IVC) (F, arrow). There are fewer cNCCs in the aorta valve leaflets in the mutant (D) compared to control embryos (C). Nuclei were counterstained with nuclear fast red. Scale bars: 100 μm.

Our studies demonstrate that conditional deletion of ETS1 in the NC recapitulates the DORV phenotype, with 50% penetrance. These results are consistent with a cell-autonomous role for ETS1 in the NC. The incomplete penetrance is likely due to variation in the precise time that ETS1 is deleted by the PAX3/Cre driver, relative to the exact time in cardiac development that ETS1 is required for normal cardiac crest migration. Normally, cardiac crest cells emigrate from the neural tube beginning at about E8.5. Our *in vivo* studies demonstrate abnormal NC migration already by E9.5, consistent with an early requirement of ETS1 for proper migration.

Our *in vitro* studies demonstrate decreased migration velocity and evidence for increased cell adhesion in ETS1 KO cultured NC cells. We subsequently determined that loss of ETS1 results in an increase in the expression of N-cadherin, a critical cell adhesion molecule required for normal NC migration. Previous studies have demonstrated that N-cadherin expression is downregulated prior to the onset of NC migration (21), and that increased N-cadherin expression impairs migration (21). Interestingly, polymorphisms in the N-cadherin gene regulatory region have been correlated with varying levels of N-cadherin expression (29). This raises the intriguing possibility that N-cadherin may be a previously unrecognized genetic modifier for the development of ventricular OFT defects.

Our studies using human NC cells derived from iPS cells from Jacobsen syndrome patients missing a copy of ETS1 and CHDs demonstrate a NC migration defect, consistent with our studies in mice. Our results also provide novel insights into why

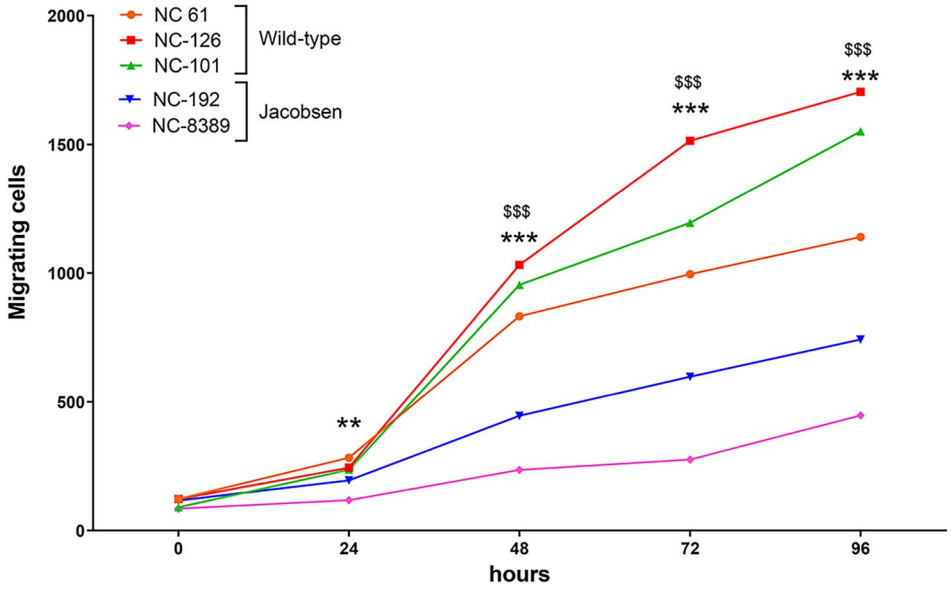

Figure 9. Effect of Ets1 reduction on NC cell migration *in vitro*. The plot shows the cell count of cells migrated in the detection zone every 24 h, for each cell lines (three NCC wild-type and two NCC Jacobsen), cultured in standard conditions. The graph shows a significant reduction of cell migration in Jacobsen lines. All the graphs were generated with GraphPad Prism. The statistical analysis was performed with ANOVA Tukey's multiparametric test; $^{**}P < 0.01$, $^{***}P < 0.001$ average wild-type vs NC 8389; $^{\$\$\$}P < 0.001$ average wild-type vs NC 192.

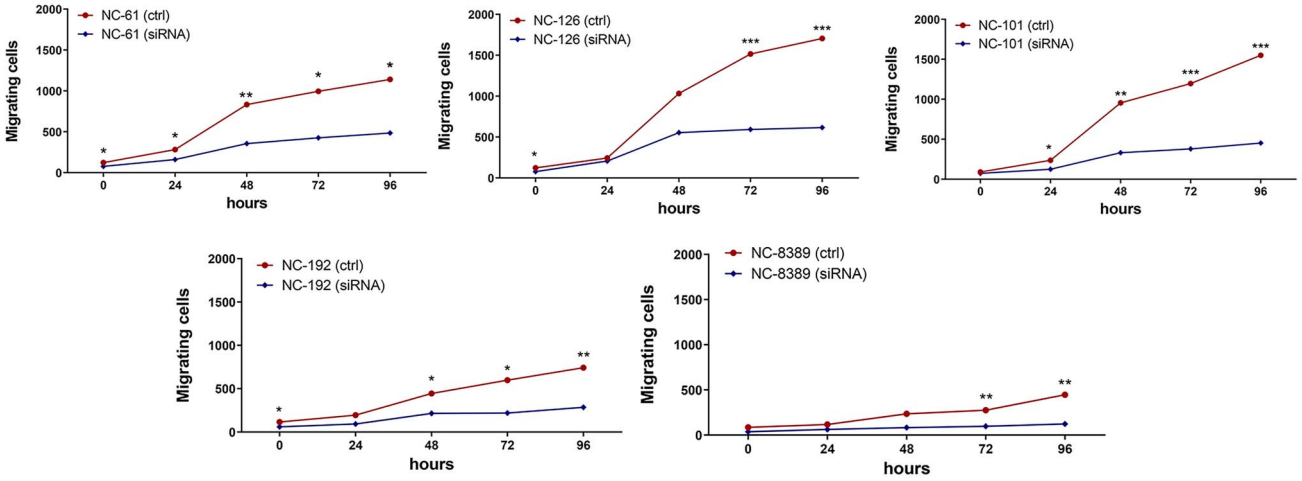

Figure 10. Migration assay for each individual line, before and after treatment with siRNA. The plot shows the cell count of cells migrated in the detection zone every 24 h, for each cell line growing in standard conditions (red lines) or silenced for ETS1 for 72 h (blue lines). The graph shows a significant reduction of cell migration when ETS1 is silenced. All the graphs were generated with GraphPad Prism. The statistical analysis was performed with ANOVA Sidak's multiparametric test; $^{*}P < 0.05$, $^{**}P < 0.01$, $^{***}P < 0.001$ siRNA vs controls for each cell line.

only homozygous KO mice exhibit DORV, while human patients with Jacobsen syndrome have CHDs with only one copy of ETS1 deleted. Specifically, we observed different ETS1 mRNA and protein levels in NC cells derived from the iPS cells from the two patients with Jacobsen syndrome and HLHS. The patient with the largest deletion, 8389, had a markedly lower level of ETS1 mRNA and protein (analogous to a mouse null mutant), compared to the controls, and the most severe migration defect. Consistent with this, the siRNA inhibition of Ets1 in the control cells reduced the number of migrating cells to that of patient 8389 NOT treated with siRNA. Patient 192, with a smaller deletion, had similar mRNA levels as controls, and an intermediate migration defect compared to patient 8389. This would suggest that in this patient, the cell migration defect may be due to decreased function of the Ets1 protein derived from the 'normal' allele, compared to the controls. In our iPSC model we observed a large effect on migration with only 10–15% of cells expressing clearly detectable levels of Ets1 protein. This suggests the intriguing possibility that Ets1+ cells lead the migration of Ets1− cells in a 3-D environment.

Taken together, our studies demonstrate a critical cell autonomous role for ETS1 in regulating early cardiac crest migration and OFT septation, advancing our understanding of the molecular and cellular basis for the pathogenesis of one anatomic variant of DORV in humans.

Limitations of the study

Our studies on global and conditional deletion mice were performed on homozygous KO mice, whereas in human patients with

JS and CHDs there is one normal ETS1 allele. As described above, patient 8389 had severely diminished ETS1 mRNA and protein levels, analogous to the mouse homozygous KO 'null' mutant. In contrast, patient 192 had mRNA and protein levels similar to controls, suggesting that the ETS1 protein encoded by the intact chromosome in this patient has diminished function. Both mechanisms may contribute to the cardiac phenotype, whereas other patients without a cardiac phenotype may have a more normal functioning allele from the intact chromosome with normal levels of mRNA and protein. Additionally, the differences between mice and humans could also be due to a lower threshold for sensitivity to the ETS gene dosage in humans than in mice.

Our *in vivo* studies on NC migration were performed on global ETS1 KO mice. Although conditional deletion of ETS1 recapitulated the DORV phenotype observed in the global KO mice, it is still possible that ETS1 regulates additional factors through a non-cell-autonomous mechanism that can contribute to the DORV phenotype. Our studies on human NCCs derived from iPS cells were performed on two patients with HLHS. Previous studies have implicated a NCC component contributing to the pathogenesis of HLHS (30). Therefore (in order to contain costs) we chose to generate iPS cells from two Jacobsen syndrome patients with HLHS to be used for the present study as well as for future studies to investigate the role of ETS1 in other cardiac cellular lineages that are also implicated in causing CHDs, such as the endocardium (31). In addition, although we did not specifically assess the aortic valve morphology in the NC conditional deletion, conditional deletion of ETS1 in the endothelium did not affect aortic valve morphology, consistent with the loss of ETS1 in the NC as the cause of the bisinuate aortic valve that we observed in the ETS1 global KO. We have demonstrated that endothelial deletion of ETS1 leads to a coronary defect and ventricular non-compaction (32). The relative contribution of ETS1 deficiency in the NC versus the endocardium in the pathogenesis of HLHS and other CHDs will continue to be an area of great interest for future studies (31).

Materials and Methods

Mice

Global ETS1 null mice have been described previously (33). Mice from the Jackson Laboratory are Pax3Cre (17) (#005549), Rosa26 tdTomato (16) (#007908) and C57BL6/J (#000664). Ets1 floxed mice were obtained from Dr Michael Ostrowski and have been reported previously (23).

Mice were maintained on a C57BL6/J background, and genotyping was performed as described. Animal care and experimental procedures were performed according to the NIH Guide for the Care and Use of Laboratory Animals as well as institutional guidelines and approved by the Institutional Animal Care and Use Committee at UC San Diego (UCSD IRB Protocol #S01049).

Immunohistochemistry and histological analyses

For immunohistochemistry, mouse embryos were dissected out in PBS and fixed in 4% paraformaldehyde overnight, then saturated with 20% sucrose and frozen in OCT component and cut into 8-μm-thick sections on a cryostat. Sections were blocked and stained with antibodies. We used antibodies to the following proteins: anti-ETS1 (Cell Signal, D808A, #14069), anti-N-cadherin (Abcam, #ab76057), anti-Sox10 (Santa Cruz Biotechnology, SC-17342) and anti-Sarcomeric alpha-actinin (Abcam, ab68167). Donkey anti-rabbit Alexa Fluor 488 secondary antibody was from Jackson ImmunoResearch Laboratories Inc. For histological analyses, mouse embryos were fixed in 4% paraformaldehyde overnight, dehydrated and embedded in paraffin, cut into 8-mm-thick sections using a microtome and stained with hematoxylin–eosin according to standard protocol.

Time-lapse imaging of migrating cNCCs in explant culture

Mouse embryos were treated by dispase to dissociate the tissue gently. After treatment, neural tubes from somite 1–3 regions (cardiac NC) were dissected out and cut into 100× 300 μm pieces. Each piece of cardiac NC tissue was placed on fibronectin-coated glass bottom slides and incubated in 5% CO_2 and 21% O_2 at 37°C for 16 h, and then the time-lapse imaging capture was initiated. The time-lapse imaging was performed at 10 min intervals for 3 h at 37°C.

X-gal staining of mouse embryos

Mouse embryos were fixed in 4% paraformaldehyde for 30 min on ice, permeabilized in PBS containing 0.02% nadeoxycholate and 0.01% NP-40 for 4 h at room temperature and were then subjected to 5-bromo-4-chloro-3-indolyl-D-galactoside (X-gal) staining.

Analysis of collagen

Sections were stained with Sirius Red/Fast Green Collagen staining kit (Chondrex Inc., #9046) according to manufacturer's protocols.

Manufacture and characterization of human iPSCs

Sendai reprogramming of primary human fibroblasts was conducted using CytoTune-iPS Sendai Reprogramming Kits according to manufacturer's instructions (Invitrogen, A13780-02, A16517, A16518) and manufactured by ReGen Theranostics. All skin biopsies were undertaken by institutional regulations. Briefly, skin biopsy samples were dissected into pieces and incubated in the six-well plate under a glass coverslip. Fibroblasts were maintained in DMEM/high glucose/glutamax (Invitrogen, 10 566-016). After 7–14 days fibroblasts were removed by TrypLE (Invitrogen, 12 604 013), washed and expanded into a 100 mm dish. After infection with Sendai 2.0 (DMEM, essential amino acids and 10% FBS) fibroblasts were cultured in E7 media (STEMCELL Technologies, 05910). Colonies were selected and expanded via mechanical dissociation and maintained in mTeSR1 on GelTrex (Thermo Fisher, purity ≥ 98%) coated plates. All clones were subjected to etoposide sensitivity assay testing, analysis of TRA-1-60 surface expression by flow cytometry, karyotyping, DNA fingerprinting and mycoplasma screening.

Generation of NC cells from iPSCs

To generate NC cells from human iPSCs, we used the neurospheres protocol, as previously described (23,24) using AggreWell system (StemCell Technologies). Briefly, stem cells were detached as single cells using Accutase, counted to calculate the necessary number of cells dependent on the size of spheres and number of wells, and transferred to the AggreWell plate. After 24 h incubation, neuralization was initiated by carefully moving the spheres to low attachment well plate in serum-free chemically defined media [1:1 ratio of DMEM/F12 glutamax (Gibco): neurobasal medium, 0.05X B27 supplement without vitamin A (Gibco), 10% BIT 9500 (StemCell Technologies), 5 μg/ml insulin (Sigma), 20 ng/ml bFGF (Chemicon), 20 ng/ml EGF (Sigma), 1 mM glutamine (Gibco)]. Half of the medium was changed every day for 5 days. Then, the neurospheres were plated on Matrigel-coated culture dishes and

allowed to migrate for 5 days in the same medium as described above, supplemented with 20 ng/ml EGF, 20 ng/ml bFGF, 5 μg/ml insulin and 5 mM nicotinamide. The medium was changed every other day. We carried out stem cell neuralization under 3% O_2 conditions.

Invasion assay

To assess the invasion ability of NC cells through an extracellular matrix we used the Oris™ Cell Migration Assay (CMA1.101, Platypus Technologies), which is based on a 96-well plate with 'stopper' barriers that create a central cell-free detection zone for cell migration. NC cells were plated in a 96-well plate coated with Matrigel in the presence of the 'stopper' tool. We seeded each cell line at the same cell density to minimize variations. For the controls, we plated cells in standard conditions (2-D Matrigel without the stopper tools) and quantified them at each time point to identify potential differences in cell proliferation rate among the lines. Cells were incubated overnight to allow attachment to the surface. The 'stopper' tool was carefully removed to create the detection zone at the center of each well and a 3-D matrix was created adding 30 μL of Matrigel, homogeneously distributed on top of the cell monolayer and solidified at 37°C for 30 min. Cell medium was added on top of the Matrigel coating. Each condition had four replicates per experiment, and each experiment was reproduced two times separately. Cell tracking was done by taking pictures in the bright field every 24 h, using an automated microscope (Celigo High Throughput Micro-Well Image Cytometer, Nexcelom) and the number of migrated cells was quantified by counting the cells in the detection zone using Celigo software. GraphPad Prism was used for plotting and statistical analysis, performed using the appropriate two-way ANOVA test as indicated in each figure. At the end of the invasion assay cells were fixed and stained with DAPI, Sox10 and ETS1, as described below.

ETS1 silencing and metalloproteinases inhibition

ETS1 silencing gene in iPSC-derived NCC was achieved by using Accell ETS1 siRNA SMARTpool (E-003887, Dharmacon) following the manufacturer's instructions. ETS1 siRNA was used at 1 μM and delivered in the NC medium. Incubation of 72 h achieved ETS1 silencing at 37°C under 3% O_2 conditions. The result of the silencing was assessed and confirmed by qPCR and immunocytochemistry. Silenced cells were then plated for the invasion assay as described above.

Immunocytochemistry

Cells were imaged at the end of the differentiation protocol from iPSC and at the end of the invasion assay as follows: Media was aspirated, and cells rinsed once with PBS for 2 min, followed by fixation with 4% PFA for 10 min at room temperature. Cells were then washed twice with PBS and blocked and permeabilized with PBSAT (0.5% Triton X-100 and 2% BSA diluted in PBS) for 1 h. Incubation with the following primary antibodies was carried out overnight: goat anti-SOX2 (1:500, R&D), rabbit anti-SOX9 (1:100, Millipore), rabbit anti-SOX10 (1:500, R&D), goat anti-Nestin (1:500, Santa Cruz Biotechnology), mouse anti-Integrin α4 (1:500, Millipore), rabbit anti-Pax3 (1:500, R&D) and rabbit anti-ETS1 (1:250, Cell Signaling). Cells were washed three times with PBSAT and then incubated with the corresponding secondary antibody in blocking solution for 1 h at room temperature. After washing three times with PBSAT, nuclei were stained with DAPI (diluted 1:000 in PBSAT) for 10 min. Cells were then washed two times with PBS and kept in PBS at 4°C until ready to be analyzed. Images were acquired using IC200 microscope (Vala Sciences) and analyzed with Acapella (PerkinElmer).

Supplementary Material

Supplementary Material is available at *HMG* online.

Acknowledgements

The authors would like to thank Dr Michael Ostrowski for providing the *Ets1* floxed mice. The authors also would like to thank the UCSD School of Medicine Microscopy Core (Grant: NINDS P30 NS047101) for their invaluable technical support.

Funding

American Heart Association (#16GRNT26700008); The Hertz Family Foundation; The Rady Children's Hospital Foundation; The 11q Research and Resource Group; The Chloe Duyck Memorial Fund; The Warren J. and Betty C. Zable Foundation and the cast and crew of 'How I Met Your Mother'.

Disclosures

The authors have no disclosures.

References

1. Creazzo, T.L., Godt, R.E., Leatherbury, L., Conway, S.J. and Kirby, M.L. (1998) Role of cardiac neural crest cells in cardiovascular development. *Annu. Rev. Physiol.*, **60**, 267–286.
2. Conway, S.J., Henderson, D.J. and Copp, A.J. (1997) Pax 3 is required for cardiac neural crest migration in the mouse: evidence from the splotch (Sp2H) mutant. *Development*, **124**, 505–514.
3. Kirby, M.L. (1989) Plasticity and predetermination of mesencephalic and trunk neural crest transplanted into the region of the cardiac neural crest. *Dev. Biol.*, **134**, 402–412.
4. Hutson, M.R. and Kirby, M.L. (2007) Model systems for the study of heart development and disease. Cardiac neural crest and conotruncal malformations. *Semin. Cell Dev. Biol.*, **18**, 101–110.
5. Waldo, K., Miyagawa-Tomita, S., Kumiski, D. and Kirby, M.L. (1998) Cardiac neural crest cells provide new insight into septation of the cardiac outflow tract: aortic sac to ventricular septal closure. *Dev. Biol.*, **196**, 129–144.
6. Anderson, R.H., Henderson, D.J. and Chaudhry, B. (2017) Development and maintenance of the arterial valves. *Eur. Heart J.*, **38**, 687–689.
7. Bruneau, B.G. and Srivastava, D. (2014) Congenital heart disease: entering a new era of human genetics. *Circ. Res.*, **114**, 598–599.
8. Garrett-Sinha, L.A. (2013) Review of Ets 1 structure, function, and roles in immunity. *Cell. Mol. Life Sci.*, **70**, 3375–3390.
9. Favier, R., Akshoomoff, N., Mattson, S. and Grossfeld, P. (2015) Jacobsen syndrome: advances in our knowledge of phenotype and genotype. *Am. J. Med. Genet. C Semin. Med. Genet.*, **169**, 239–250.
10. Ye, M., Coldren, C., Liang, X., Mattina, T., Goldmuntz, E., Benson, D.W., Ivy, D., Perryman, M.B., Garrett-Sinha, L.A. and Grossfeld, P. (2010) Deletion of ETS-1, a gene in the Jacobsen syndrome critical region, causes ventricular septal defects and abnormal ventricular morphology in mice. *Hum. Mol. Genet.*, **19**, 648–656.
11. Davidson, B. (2007) Ciona intestinalis as a model for cardiac development. *Semin. Cell Dev. Biol.*, **18**, 16–26.

12. Alvarez, A.D., Shi, W., Wilson, B.A. and Skeath, J.B. (2003) pannier and pointedP2 act sequentially to regulate Drosophila heart development. *Development*, **130**, 3015–3026.
13. Glessner, J.T., Bick, A.G., Ito, K., Homsy, J., Rodriguez-Murillo, L., Fromer, M., Mazaika, E., Vardarajan, B., Italia, M., Leipzig, J. *et al.* (2014) Increased frequency of de novo copy number variants in congenital heart disease by integrative analysis of single nucleotide polymorphism array and exome sequence data. *Circ. Res.*, **115**, 884–896.
14. Gao, Z., Kim, G.H., Mackinnon, A.C., Flagg, A.E., Bassett, B., Earley, J.U. and Svensson, E.C. (2010) Ets1 is required for proper migration and differentiation of the cardiac neural crest. *Development*, **137**, 1543–1551.
15. Ye, M., Yin, Y. and Fukatsu, K. (2016) Evidence that deletion of ETS-1, a gene in the Jacobsen Syndrome (11q-) cardiac critical region, causes congenital heart defects through impaired cardiac neural crest cell function. In Nakanishi, T., Markwald, R.R., Baldwin, H.S., Keller, B.B., Srivastava, D. and Yamagishi, H. (eds), *Etiology and Morphogenesis of Congenital Heart Disease: From Gene Function and Cellular Interaction to Morphology [Internet]*. Springer, Tokyo, Chapter 52.
16. Madisen, L., Zwingman, T.A., Sunkin, S.M., Oh, S.W., Zariwala, H.A., Gu, H., Ng, L.L., Palmiter, R.D., Hawrylycz, M.J., Jones, A.R. *et al.* (2010) A robust and high-throughput Cre reporting and characterization system for the whole mouse brain. *Nat. Neurosci.*, **13**, 133–140.
17. Engleka, K.A., Gitler, A.D., Zhang, M., Zhou, D.D., High, F.A. and Epstein, J.A. Insertion of Cre into the Pax3 locus creates a new allele of Splotch and identifies unexpected Pax3 derivatives. *Dev. Biol.*, **280**, 396–406.
18. Betancur, P., Bronner-Fraser, M. and Sauka-Spengler, T. (2010) Genomic code for Sox10 activation reveals a key regulatory enhancer for cranial neural crest. *Proc. Natl. Acad. Sci. U. S. A.*, **107**, 3570–3575.
19. Epstein, J.A., Li, J., Lang, D., Chen, F., Brown, C.B., Jin, F., Lu, M.M., Thomas, M., Liu, E., Wessels, A. *et al.* (2000) Migration of cardiac neural crest cells in Splotch embryos. *Development*, **127**, 1869–1878.
20. Punovuori, K., Malaguti, M. and Lowell, S. (2021) Cadherins in early neural development. *Cell. Mol. Life Sci.*, **78**, 4435–4450.
21. Taneyhill, L.A. and Schiffmacher, A.T. (2017) Should I stay or should I go? Cadherin function and regulation in the neural crest. *Genesis*, **55**, 10.
22. Menendez, L., Kulik, M.J., Page, A.T., Park, S.S., Lauderdale, J.D., Cunningham, M.L. and Dalton, S. (2013) Directed differentiation of human pluripotent cells to neural crest stem cells. *Nat. Protoc.*, **8**, 203–212.
23. Cimadamore, F., Curchoe, C.L., Alderson, N., Scott, F., Salvesen, G. and Terskikh, A.V. (2009) Nicotinamide rescues human embryonic stem cell-derived neuroectoderm from parthanatic cell death. *Stem Cells*, **27**, 1772–1781.
24. Curchoe, C.L., Maurer, J., McKeown,S.J., Cattarossi, G., Cimadamore, F., Nilbratt, M., Snyder, E.Y., Bronner-Fraser, M. and Terskikh, A.V. (2010) Early acquisition of neural crest competence during hESCs neuralization. *PLoS One*, **5**, e13890.
25. Lee, G., Chambers, S.M., Tomishima, M.J. and Studer, L. (2010) Derivation of neural crest cells from human pluripotent stem cells. *Nat. Protoc.*, **5**, 688–701.
26. Anderson, R.H., Mori, S., Spicer, D.E., Brown, N.A. and Mohun, T.J. (2016) Development and morphology of the ventricular outflow tracts. *World J. Pediatr. Congenit. Heart Surg.*, **7**, 561–577.
27. McGoon, D.C., Rastelli, G.C. and Wallace, R.B. (1970) Discontinuity between right ventricle and pulmonary artery: surgical treatment. *Ann. Surg.*, **172**, 680–689.
28. Gandhi, S., Ezin, M. and Bronner, M.E. (2020) Reprogramming axial level identity to rescue neural crest-related congenital heart defects. *Dev. Cell*, **53**, 300–315.
29. Ruedel, A., Stark, K., Kaufmann, S., Bauer, R., Reinders, J., Rovensky, J., Blazicková, S., Oefner, P.J. and Bosserhoff, A.K. (2014) N-cadherin promoter polymorphisms and risk of osteoarthritis. *FASEB J.*, **28**, 683–691.
30. Ahola, J., Koivusalo, A., Sairanen, H., Jokinen, E., Rintala, R.J. and Pakarinen, M.P. (2009) Increased incidence of Hirschsprung's disease in patients with hypoplastic left heart syndrome—a common neural crest-derived etiology? *J. Pediatr. Surg.*, **44**, 1396–1400.
31. Grossfeld, P., Nie, S., Lin, L., Wang, L. and Anderson, R.H. (2019) Hypoplastic left heart syndrome: a new paradigm for an old disease? *J. Cardiovasc. Dev. Dis.*, **6**, 10.
32. Wang, L., Lin, L., Qi, H., Chen, J. and Grossfeld, P. (2022) Endothelial loss of ETS1 impairs coronary vascular development and leads to ventricular non-compaction. *Circ. Res.*, doi: 10.1161/CIRCRESAHA.121.319955
33. Barton, K., Muthusamy, N., Fischer, C., Ting, C.N., Walunas, T.L., Lanier, L.L. and Leiden, J.M. (1998) The Ets-1 transcription factor is required for the development of natural killer cells in mice. *Immunity*, **9**, 555–563.